HNPS Advances in Nuclear Physics

Vol 28 (2021)

HNPS2021

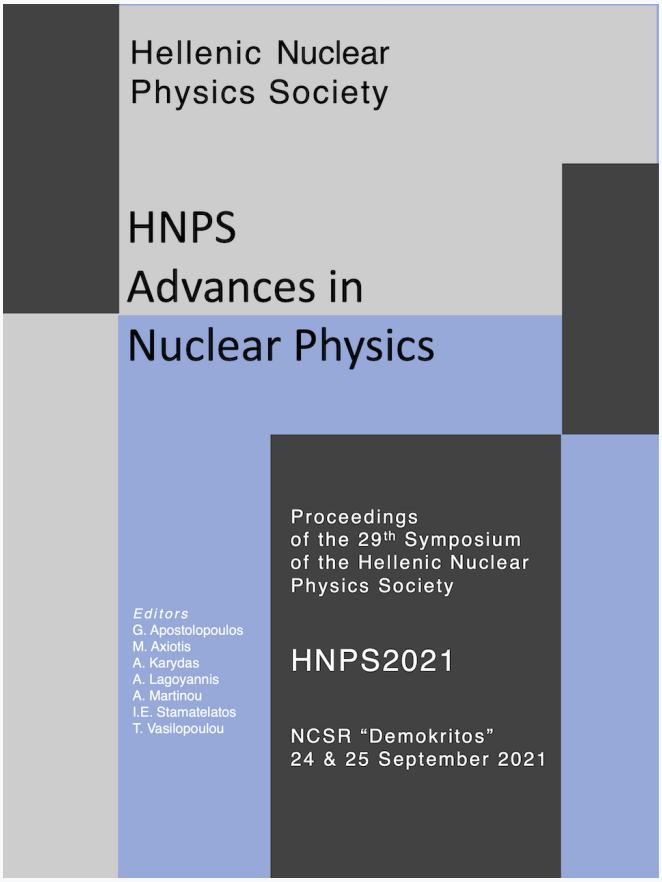

Rapid uniform rotation of proto-neutron stars, hot neutron stars, and neutron star merger remnants: The role of the temperature

Polychronis Stylianos Koliogiannis Koutmiridis

doi: 10.12681/hnps.3576

To cite this article:

Koliogiannis Koutmiridis, P. S. (2022). Rapid uniform rotation of proto-neutron stars, hot neutron stars, and neutron star merger remnants: The role of the temperature. *HNPS Advances in Nuclear Physics*, *28*, 280–285. https://doi.org/10.12681/hnps.3576

Rapid uniform rotation of proto-neutron stars, hot neutron stars, and neutron star merger remnants: The role of the temperature

P.S. Koliogiannis*

Department of Theoretical Physics, Aristotle University of Thessaloniki, 54124, Greece

Abstract Hot and dense nuclear matter and the equation of state is mandatory for studying proto-neutron stars and neutron star merger remnants. The applied equations of state are derived within the momentum-dependent interaction model and state-of-the-art microscopic data, to fulfill the thermodynamic laws. The matter is constructed under the assumptions of finite temperature and beta-equilibrium state, and finite entropy per baryon and varying values of proton fraction. Afterwards, we study the effects of finite temperature and rotation at the mass-shedding limit on the neutron stars properties, including the mass and radius, the moment of inertia, the frequency, the Kerr parameter, the central baryon density, etc. The interplay between the temperature and rotation for proto-neutron stars and neutron star merger remnants may shed light in the construction of the equation of state of nuclear matter and apply robust constraints.

Keywords Neutron stars, nuclear matter, hot equation of state, binary neutron star merger remnant

INTRODUCTION

The dynamical evolution of proto-neutron stars, the formation of black holes, as well as the post-merger compact object of a binary neutron star system, depend sensitively on the equation of state (EoS) of dense nuclear matter and, on the temperature, the proton fraction, and the possible neutrino trapped in the interior of the star. The latter indicates the need of knowing the EoS at extreme conditions of several times the normal nuclear density and temperature [1-2].

The post-merger remnant, the maximum stable mass, the spin period, as well as the lifetime of the star, depend sensitively on the dense nuclear matter properties and the high values of temperature, and are explicitly connected with the high-density region of the EoS. More specific, the high-density profile of the EoS is constrained mainly through the astrophysical observations of non/slow rotating neutron stars. In particular, the most robust ones include the PSR J0740+6620 with $M = 2.14\ M_{\odot}$ [3], which defines the lower limit for neutron star mass, and the spin frequency, which at the moment is at 716 Hz [4], through the observation of the pulsar PSR J1748-244ad. Furthermore, the intermediate along with the high-density region is also constraint through the observations of binary neutron star and black-hole neutron star mergers. In fact, the GW170817 [5] and GW190425 [6] events, have assist in narrowing the radius of the neutron star through the measurements of the tidal deformability.

THERMAL PROFILE OF THE EQUATION OF STATE

Hot neutron star matter is described by the momentum-dependent interaction (MDI) model [7] and the microscopic data provided by Akmal et al. [8] for the APR-1 EoS (hereafter MDI+APR1). The schematic presentation of the symmetric nuclear matter (SNM), the pure neutron matter (PNM), and the data of Akmal et al. [8] are presented in Figure 1. In particular, the parameterization for the cold matter is the basis for the construction of ten isothermal EoSs based on temperatures in the range [1,60] MeV, and nine isentropic EoSs based on lepton fractions and entropies per baryon in the ranges [0.2,0,4] and [1,3]k_B, respectively.

* Corresponding author: pkoliogi@physics.auth.gr

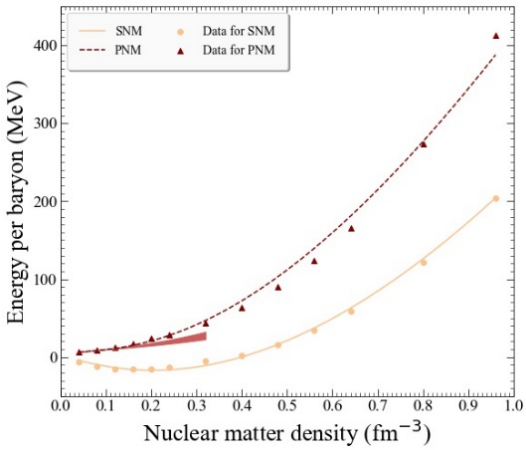

Fig. 1. *The fits of SNM and PNM of MDI+APR1 cold EoS. The SNM is presented by the circles and solid line, while the PNM is presented by the triangles and dashed line. The shaded region corresponds to benchmark calculations of the energy per particle of PNM extracted from Piarulli et al. [13].*

Concerning the solid crust region, we adopted the EoSs of Feynman et al. [9] and Baym et al. [10], while for the finite temperature/entropy and lepton fraction cases, as well as the low-density region ($n_b \leq 0.08$ fm^{-3}), the EoSs of Lattimer and Swesty [11] and the specific model corresponding to the incomprehensibility modulus at the saturation density of SNM $K_s = 220$MeV are used (https://www.stellarcollapse.org). For more information about the construction of the EoSs and their application, see Ref. [12].

An important quantity for studying the properties of neutron stars at finite temperature, is the free energy per particle, which is also directly related to the calculation of the proton fraction. In Figures 2 we display the free energy per particle and the proton fraction as functions of the baryon density for isothermal EoSs. In Figure 2, case (a) corresponds to the PNM and case (b) corresponds to the SNM. In all cases (free energy and proton fraction), due to the quantum character of hadronic matter, thermal effects manifest at low densities, where at high densities the system is more symmetric and the EoSs are converging.

Furthermore, in isentropic EoS we can study the stiffness and the stability of proto-neutron stars with the adiabatic index, and the speed of sound, defined as [1]

$$\Gamma = \frac{n}{P}\frac{\partial P}{\partial n}\bigg|_S \quad and \quad \frac{c_S}{c} = \sqrt{\frac{\partial P}{\partial E}\bigg|_S} \tag{1}$$

where P and E are the pressure and energy density, respectively. In Figure 4(a) we display the adiabatic index as a function of the baryon density for isentropic EoSs. Assuming a constant lepton fraction, the increase of the entropy per baryon leads to lower values of the central baryon density at which the maximum mass appears. In Figure 4(b) we display the square speed of sound in units of speed of light as a function of the baryon density. In this case, all EoSs never exceed the causality limit. The latter is a direct consequence of the MDI model and one of its major advantages.

UNIFORM ROTATION AND BULK NEUTRON STAR PROPERTIES

The dimensionless moment of inertia, which provides important information about the structure

of neutron stars, is displayed in Figures 5(a,b) as a function of the compactness parameter[1] for (a) isothermal and (b) isentropic neutron stars. In general, the introduction of temperature has the effect to produce lesser compact objects than the cold neutron star, in addition to lower values of dimensionless moment of inertia.

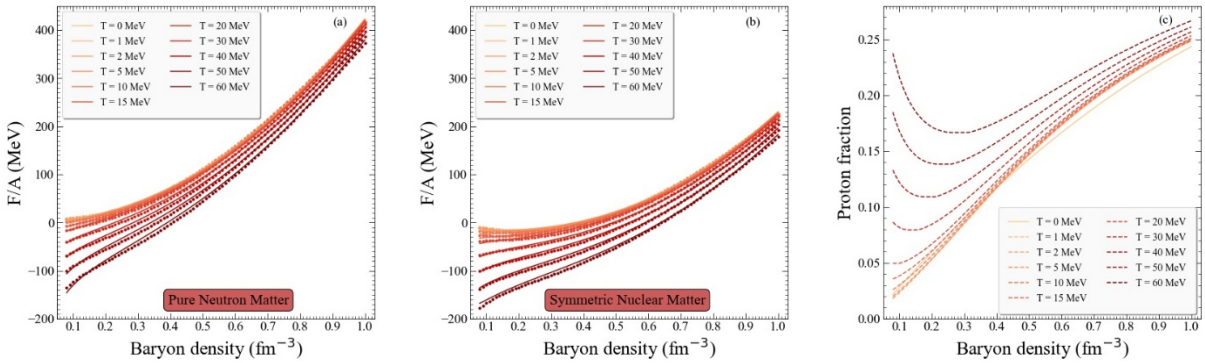

Fig. 2. *The free energy per particle as a function of the baryon density for (a) PNM and (b) SNM and isothermal EoSs. Fits are presented with the solid lines and data with circles. (c) The proton fraction as a function of the baryon density for isothermal EoSs. The cold configuration is presented with the solid line, while hot configurations are presented with the dashed lines (see also Ref. [9]).*

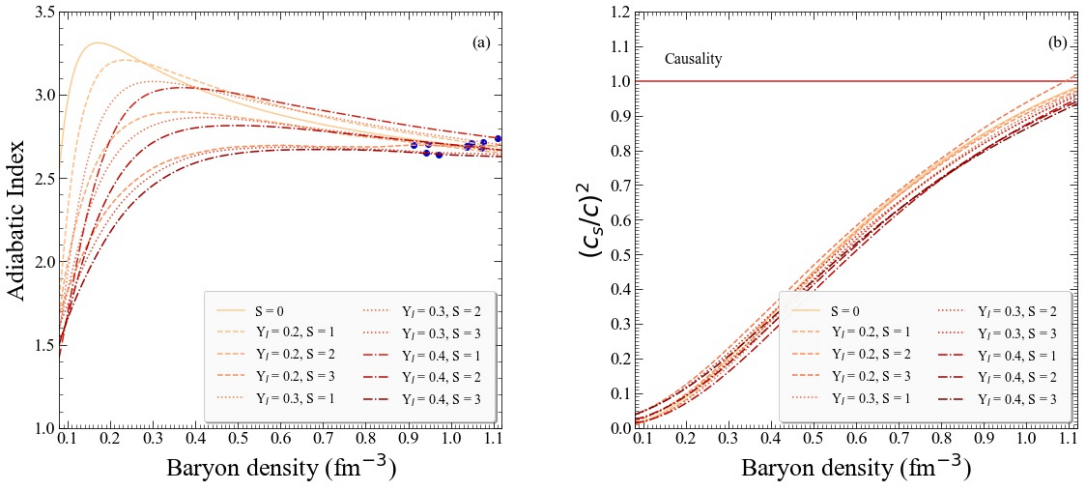

Fig. 4. *(a) Adiabatic index as a function of the baryon density for isentropic EoSs. Blue circles represent the central baryon density at which the maximum mass configuration appears. (b) Square speed of sound in units of speed of light as a function of the baryon density for isentropic EoSs. In both Figures, the cold configuration is presented with the solid line.*

The Kerr parameter[2] is a quantity related both to neutron stars and Kerr black holes, and an indicator of the final fate of the collapse of a rotating compact object. More specific, constraints for Kerr black holes are provided through the limit of Ref. [14], while the ones for neutron stars are available through the relations of angular velocity and moment of inertia in Refs. [15,16], where the limit $0.66 \leq K_{\max} \leq 0.76$ is introduced [12]. Figures 5(c,d) display the Kerr parameter as a function of the gravitational mass for (c) isothermal and (d) isentropic neutron stars. The effect of the temperature is to decrease the values of the Kerr parameter. Thus, the constraints for neutron stars and

[1] Compactness parameter: $\beta = GM/Rc^2$
[2] Kerr parameter: $K = cJ/GM^2$

Kerr black holes cannot be violated.

The angular velocity is displayed in Figures 5(e,f) as a function of the ratio of kinetic to gravitational binding energy T/W for (e) isothermal and (f) isentropic neutron stars. A possible way for a neutron star to emit gravitational waves is through the instabilities driven by gravitational radiation. Precisely, the point that locates these non-axisymmetric instabilities is set at $T/W = 0.08$ for models with $M = 1.4\,M_{\odot}$ [17]. While the effect of temperature is to avoid suck kind of instabilities, for low temperatures, the instability will set in before the mass-shedding limit is reached. In this case, the maximum gravitational mass, as well as the angular velocity, will be lowered for the neutron star.

The above analysis will be useful to provide relevant constraints for the aftermath of a binary neutron star merger, which is a compact object that rotating differentially with neutron star matter. However, in this case, we consider a uniform rotating isothermal remnant of a temperature at 30 MeV or an isentropic one with $S = 1$ and $Y_l = 0.2$. Uniform rotation approach will be able to provide useful constraints at the mass-shedding limit and the maximum mass configuration. In particular,

$$\beta_{\mathrm{rem}}^{\mathrm{iso}} \leq 0.19 \text{ and } \beta_{\mathrm{rem}}^{\mathrm{ise}} \leq 0.27,$$
$$K_{\mathrm{rem}}^{\mathrm{iso}} \leq 0.42 \text{ and } K_{\mathrm{rem}}^{\mathrm{ise}} \leq 0.68,$$
$$(T/W)_{\mathrm{rem}}^{\mathrm{iso}} \leq 0.19 \text{ and } (T/W)_{\mathrm{rem}}^{\mathrm{ise}} \leq 0.27,$$

where the superscripts “iso” and “ise”, correspond to isothermal and isentropic profiles. Therefore, if the aftermath of a binary neutron star merger is an isothermal object, it is a lesser compact object than the cold neutron star with lower values of maximum gravitational mass and frequency, and stable toward dynamical instabilities. In the case that is an isentropic object, the maximum gravitational mass, as well as the angular velocity are comparable to the cold neutron star. In addition, it is unstable toward the dynamical instabilities [12].

CONCLUDING REMARKS

Thermal effects in isolated neutron stars and binary neutron star merger remnants have been analyzed under thermodynamically consistent EoSs (isothermal and isentropic), and nonrotating and uniformly rotating at the mass-shedding limit axisymmetric equilibrium sequences. The EoSs and their application is acceptable for a first-order study of proto-neutron stars, hot neutron stars, as well as binary neutron star merger remnants that have survived the dynamical and strongly non-axisymmetric post-merger evolution and settled down into a stable quasi-equilibrium state [18].

The applied nuclear model for the construction of the EoSs, presents merits compared to other models: (a) the thermal effects have been included in a self-consistent way, (b) the model produce a wide range of EoSs by properly modifying the density dependence of the symmetry energy, (c) the model reproduces microscopic calculations concerning both the SNM and the PNM, (d) the momentum dependence of the potential interaction is in accordance with the terrestrial studies and experiments of heavy-ion reactions for both low and high densities and temperatures, and (e) the model ensures the causal behavior of the EoS at high densities.

Moment of inertia informs us about the structure of the neutron star as it continuously changes its angular velocity and loses angular momentum due to radiation. Thermal support led to the conclusion that moment of inertia, and compactness parameter, have lower values than the cold neutron star. This behavior is influenced by the unique interplay between the gravitational mass and the equatorial radius.

In the case of the Kerr parameter, as the maximum value is set via the cold configuration, thermal support cannot lead a star, constrained to mass-energy and momentum conservation, to collapse into a

maximally rotating Kerr black hole.

Fig. 5. *(a,b) Dimensionless moment of inertia as a function of the compactness parameter. (c,d) Kerr parameter*

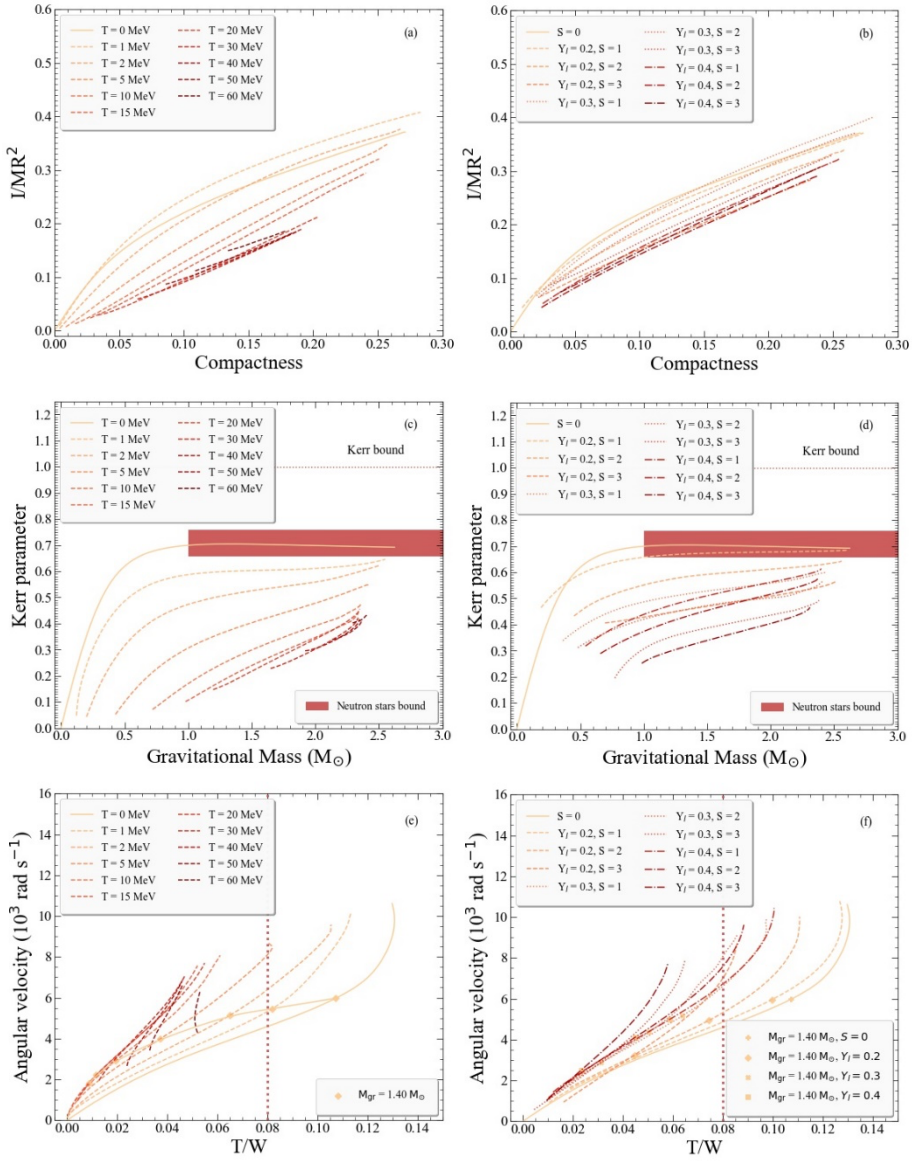

as a function of the gravitational mass. Shaded region corresponds to neutron star constraints, and the dotted horizontal line is the Kerr black hole limit, $K_{B.H.} = 0.998$. *(e,f) Angular velocity as a function of the* T/W. *The vertical dotted line marks the limit* $T/W = 0.08$. *The markers correspond to the* $M = 1.4\ M_{\odot}$ *configuration. All Figures correspond to the mass-shedding limit, where Figures (a,c,e) correspond to isothermal neutron stars, and (b,d,f) correspond to isentropic neutron stars.*

In the ratio of T/W, thermal support is responsible for the lower values than the cold neutron star. In this case, the instabilities originated from the gravitational radiation never occur in a hot and rapidly rotating neutron stars, or in a post-merger remnant. However, in cases where the ratio exceeds the $T/W = 0.08$, this value sets the limit for the maximum gravitational mass and angular velocity, lowering the latter quantities for the neutron star.

For the numerical integration of the equilibrium equations, we used the publicly available numerical code *nrotstar* from the C++ Lorene/Nrotstar library (for more details see Ref. [19]; for the instability criteria see Ref. [12] and references therein).

References

[1] M. Prakash, I. Bombaci, M. Prakash, P.J. Ellis, J.M. Lattimer, R. Knorren, Phys. Rep. 280, 1 (1997)
[2] J.O. Goussard, P. Haensel, J.L. Zdunik, Astron. Astrophys. 321, 822 (1997)
[3] H. Cromartie, E. Fonseca, S. Ransom, P.B. Demorest, Z. Arzoumanian et al., Nat. Astron. 4, 72 (2020)
[4] J.W.T. Hessels, S.M. Ransom, I.H. Stairs, P.C.C. Freire, V.M. Kaspi, and F. Camile, Sci. 311, 1901 (2006)
[5] B.P. Abbott, R. Abbott, T.D. Abbott et al., Phys. Rev. Lett. 119, 161101 (2017)
[6] B.P. Abbott, R. Abbott, T.D. Abbott et al., Astrophys. J. 892, L3 (2020)
[7] C.C. Moustakidis, C.P. Panos, Phys. Rev. C 79, 045806 (2009)
[8] A. Akmal, V.R. Pandharipande, D.G. Ravenhall, Phys. Rev. C 58, 1804 (1998)
[9] R.P. Feynman, N. Metropolis, E. Teller, Phys. Rev. 75, 1561 (1949)
[10] G. Baym, C. Pethick, P. Sutherland, Astrophys. J. 170, 299 (1971)
[11] J.M. Lattimer, F.D. Swesty, Nucl. Phys. A 535, 331 (1991)
[12] P.S. Koliogiannis, C.C. Moustakidis, Astrophys. J. 912, 69 (2021)
[13] M. Piarulli, I. Bombaci, D. Logoteta, A. Lovato, R.B. Wiringa, Phys. Rev. C 101, 045801 (2020)
[14] K.S. Thorne, Astrophys. J. 191, 507 (1974)
[15] P.S. Koliogiannis, C.C. Moustakidis, Phys. Rev. C 101, 015805 (2020)
[16] D.S. Shao, S.P. Tang, X. Sheng, J.L. Jiang, Y.Z. Wang, Z.P. Jin, Y.Z. Fan, D.M. Wei, Phys. Rev. D 101, 063029 (2020)
[17] S.M. Morsink, N. Stergioulas, S.R. Blattnig, Astrophys. J. 510, 854 (1999)
[18] J.D. Kaplan, C.D. Ott, E.P. O'Connor, K. Kiuchi, L. Roberts, M. Duez, Astrophys. J. 790, 19 (2014)
[19] LORENE, Lorene: Langage objet pour la relativité numérique, http://lorene.obspm.fr/ (1998)